HEFAT2008
6th International Conference on Heat Transfer, Fluid Mechanics and Thermodynamics
30 June to 2 July 2008
Pretoria, South Africa
Paper number:AU1

ANALYSIS OF FLOW STRUCTURES AND NEAR WALL BEHAVIOR OF FLUID FLOW AND LOCAL HEAT TRANSFER IN HEAT EXCHANGERS WITH INCLINED FLAT TUBES

Ahrend U.* and Koehler J.
*Author for correspondence
Institut fuer Thermodynamik,
Technical University Braunschweig,
38106 Braunschweig,
Germany,
E-mail: u.ahrend@tu-bs.de

ABSTRACT

Compact flat tube heat exchangers with inclined refrigerant tubes and plane fins are studied at Reynolds numbers based on the hydraulic diameter of Re_{dh}=3900 and Re_{dh}=2500. The fluid field is measured parallel to the fins and the wall distance is varied. The fluid movement and particularly the change of fluid movement close to the fin are examined.

A steady two dimensional CFD simulation is developed to provide an efficient model for geometric optimization. The model is validated by experimental flow measurements.

This paper also compares the local heat transfer distribution on the fin with near wall PIV measurements and seeks relations between certain flow structures and enhanced heat transfer.

Shadowing effects prevent the examination of instantaneous velocity fields in the named geometries. The gappy proper orthogonal decomposition (Gappy POD) is tested for the reconstruction of instantaneous velocity data in shadowed region.

INTRODUCTION

Heat exchanger devices tend to become smaller and smaller. This is particularly true for mobile applications whith a great demand for compact and efficient heat exchangers. These heat exchangers are characterized by a high heat transfer power in a small volume. The increase of heat transfer performance goes along with a dramatic size reduction and increase of the ratio between heat transferring surface and fluid volume.

In automobile applications most heat exchangers use flat tubes and an advanced fin technology to satisfy the goals of compactness and efficiency. If we consider complete systems consisting of ventilator and heat exchanger the greatest competitor of heat transfer performance are viscous or pressure losses that usually rise when fin density increases. Overall performance correlations are often used to study and describe the properties of the named heat exchangers. Despite the great success in surface technology in the past decades it is accepted that only a local description of flow and heat transfer in complex flow passages can lead to further improvement.

A combined analysis of flow features and heat transfer distribution is necessary to analyze the quite complex interaction and improve the design of heat transferring devices.

Another severe problem in heat exchangers with high fin densities is the drainage of condensed water if we consider air/liquid heat exchanger. This becomes important in air conditioning applications where the heat exchanger is used as an evaporator. Unfortunately, the widely used flat tubes show a quite poor performance as far as water drainage is concerned.

The concept studied in this paper examines heat exchangers using horizontally inclined flat tubes (cf. Figure 1). The inclination of the tubes may have two advantages: First, the inclination eases the drainage of water and, secondly, it can be used to guide and influence the air flow through the tubes. The arrangement of the tubes has the potential to promote lateral mixing of fluid and thereby increase heat transfer. This would allow reducing the fin density and, consequently, avoiding the risk of water blockage etc.

The model examined in this paper has a constant inclination angle of 20°. Further studies and a combined analysis of heat transfer and pressure loss may reveal that lower angles or even different angles for each of the tube rows yield the best performance. This optimization process has to be carried out numerically due to the complexity and time consumption of experiments. In this paper a 2D numerical model is presented and validated by measurement data that can be used within an optimization process.

The tube arrangement sets up quite severe problems particularly for PIV measurements of the fluid flow. Most dominant

are shadowing effects due to the inclination of the tubes. The need for a high intensity light sheet and a homogeneous illumination throughout the measurement region cannot be satisfied in the here studied geometries. Even though the tubes are made of Perspex a strong curvature of the material creates shadows occurring underneath the tubes.

The problem may be circumvented in parts by the superposition of averaged velocity fields measured at different light sheet angles. However, this procedure only holds for averaged data. Once we want to get instantaneous data in the whole measurement region not obscured by shadows we cannot apply the superpositioning procedure.

A solution to this problem based on the gappy proper orthogonal decomposition will be examined in this paper.

NOMENCLATURE

$\vec{u}(\vec{x})$	[m/s]	Velocity field
u,v,w	[m/s]	Components of the velocity field in x–, y–, z–direction
x,y,z	[m]	Cartesian coordinates
x	[m]	Streamwise direction
z	[m]	Fin normal direction
$\vec{x}$	[m]	Cartesian vector
$\overset{*}{\vec{u}}(\vec{x})$	[m/s]	Gappy velocity field
$\widetilde{\vec{\varphi}}^{(i)}(\vec{x})$	[]	Intermediate spatial POD basis function
$\tilde{a}^{(i+1)}(n)$	[m/s]	Intermediate expansion coefficient
Nu	[]	Nusselt number
Special characters		
b	[m]	Lateral fin spacing
$b_{1/2}$	[m]	Half lateral fin spacing
s_l	[m]	Tube spacing in streamwise (x–) direction
s_q	[m]	Tube spacing in lateral (y–) direction

MODEL DESCRIPTION

Two models of a flat tube heat exchanger with inclined tube arrangement have been built from Perspex in order to provide optical access for laseroptical measurements. A sketch of the model is shown in Figure 1**.**

It consists of just one flow passage between two parallel fins. The spacing of the fins is b.

One model is designed for a wind tunnel in which the heat transfer measurements by means of the ammonia absorption method (AAM) are performed. The second one is used for particle image velocimetry (PIV) measurements.

In contrast to real applications in automobile evaporators e.g. the experimental model has to be scaled up. This is necessary to allow measurements with conventional PIV technique and decent resolution. The streamwise separation of the tubes is s_l=40mm in the case of the PIV model and s_l=24mm in the case of the AAM model. The distance s_l is also identical to the length of the flat tube. The thickness of a tube is $1/4s_q$. The ratio between lateral and streamwise separation of the tubes is s_l/s_q=1.259 for both models. Geometrical and dynamical similarity between both models is ensured throughout all measurements. The used coordinate system is defined in Figure 1.

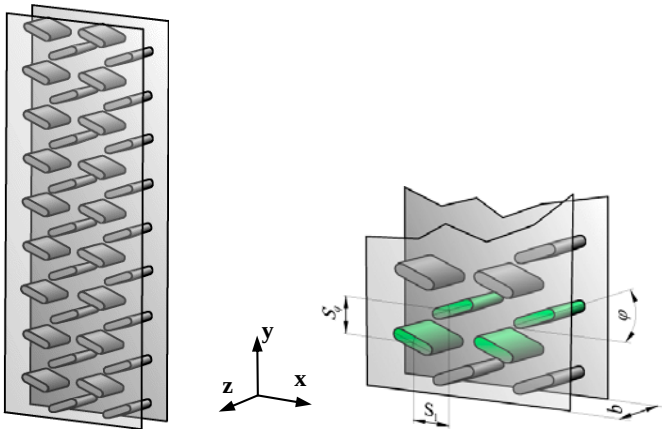

Figure 1 Model of the flat tube heat exchanger with inclined tubes. The right picture magnifies a selected region within the device. The green shaded tubes constitute a periodic cell. S_q is the lateral spacing of the tubes and s_l is the separation in streamwise direction.

FLUID FLOW MEASUREMENTS

The fluid flow in the named device is carried out by means of the PIV technique. The interrogation areas are 32x32 pixels with an overlap of 50%. Ensembles of 200 double pictures are used for all evaluations.

The laser light sheet is placed parallel to the fins, i.e. the x-y plane. The distance of the sheet to the wall is varied. For closer wall distances a pronounced reflection of the wall deteriorates the quality of PIV measurements and yields very poor data. In order to circumvent the deleterious reflections a fluorescent Rhodamine containing painting is applied to the walls. Reflected light is absorbed by this painting and shifted towards higher wavelengths. A band pass filter allowing only the signal wavelength at 532nm to pass filters out the malicious light coming from the wall. Details to this procedure can also be found in [1].

The raw data is evaluated by commercial PIV software. The post–processing of the vector maps is done by means of the visualization tool OpenDX.

Discussion of the Fluid Flow

The fluid flow is studied in the x–y plane at a wall distance of $z/b_{1/2}$=1 and $z/b_{1/2}$=0.1. The Re number based on the hydraulic diameter is Re_{dh}=3900.

Figure 2 shows the magnitude of the averaged velocity field and some corresponding streamlines within the flat tube geometry in the middle of the channel at $z/b_{1/2}$=1. The picture is a superposition of six different PIV measurements, i.e. six different light sheet positions have been used to illuminate most of the shown area. This procedure is necessary due to multiple shadows created by the tubes. They do not allow sufficient illumination (cf. left picture in Figure 9) and have to be excluded from further evaluation. For each light sheet position the mean velocity field is calculated and then superimposed by the other measurements. In regions where we have two light sheets contributing data to the same spot it is filled by the average velocity value of the two data sets.

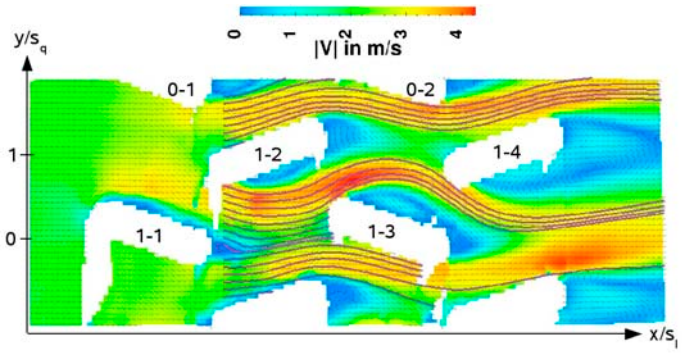

Figure 2 Map of the mean velocity field within the flat tube heat exchanger at Re_{dh}=3900 and $z/b_{1/2}$=1. Streamlines indicate the wave like flow of fluid through the device.

Figure 2 shows that the fluid is accelerated within the geometry. It enters at a velocity of about 2m/s and reaches velocities far beyond 3m/s. This is caused by the blockage of the tubes.

We also find wake regions behind the tubes. They increase in size as we pass farther downstream. The fluid is able to follow the tubes only at the very first tube row. Soon at the second row separation occurs. Closer views show the fluid attaching again at the rear part of the tubes belonging to the second tube row. We do not find reattachment farther downstream. The curvature of the streamlines is increasing in downstream direction.

The streamlines also indicate that major parts of the fluid are forced to follow a wave like path through the geometry. There are two groups of streamlines that show a different behavior: Streamlines passing between tubes 0-1, 0-3 and 1-2, 1-4 (cf Figure 2) are quite smooth and show only a slight curvature. They are subsequently referenced as group A. The second group of streamlines passing through 1-2, 1-4 and 1-1, 1-3 is much more influenced by the presence of the tubes. These streamlines exhibit a much stronger curvature. They are called group B.

Both groups of streamlines seem to form quite stable wave like flow channels, i.e. there are no streamlines of group B joining those of group A. This indicates that despite the strong lateral movement within a flow channel there is no mixing between adjacent channels.

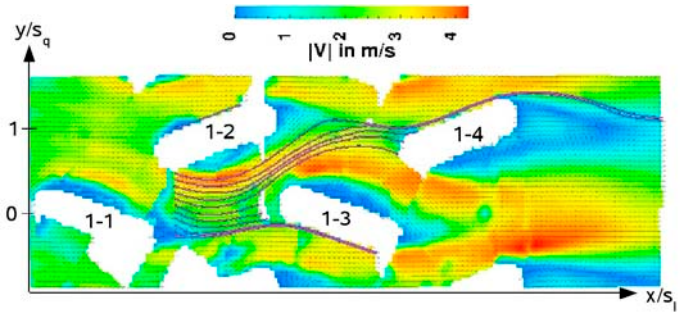

Figure 3 Map of the mean velocity field within the flat tube heat exchanger at Re_{dh}=3900 and $z/b_{1/2}$=0.1. The drawn streamlines indicate a pronounced lateral movement.

This behavior changes if we analyze the flow field at closer wall distance. The mean velocity field at Re_{dh}=3900 and a wall distance of $z/b_{1/2}$=0.1 is displayed in Figure 3. We find that the shape of the wake regions changes slightly compared to $z/b_{1/2}$=1. The major difference is the behavior of the streamlines. If we concentrate on the region between tube 1-2 and 1-3 in Figure 3 we find that major parts of the fluid do no longer stay in their wave like channel between tubes 1-2, 1-4 and 1-1, 1-3 as in Figure 2. Contrarily, they leave their passage and join the upper flow channel. This fact shows that there is indeed a lateral mixing between adjacent channels but only close to the fin. It may be favorable for an increased heat transfer.

NUMERICAL ANALYSIS

A numerical description of fluid flow within the flat tube heat exchanger is desired to allow an automated optimization process of the geometry for future work. The goal will be to combine grid generation, CFD simulation and optimization in an automated scheme. First results and studies of the feasibility of this approach have been published in [2].

In order to start with an optimization procedure we need to validate the numerical model by means of experimental reference data. The afore described results provide the necessary fluid flow and pressure data to test the numerical model.

The commercial code Fluent 6.3 is used to solve the velocity and temperature field for the two-dimensional problem. The Reynolds number is identical to the PIV measurements, namely Re_{dh}=3900. Periodic boundary conditions are used in y–direction thereby exploiting the periodicity of the geometry.

Time efficiency will be a crucial point in practical applications. Therefore, we seek for a steady solution of the flow. However, we have to keep in mind that experiment tells us that there are regions in the flow which show unsteady behavior. In order to achieve a stationary solution the following scheme is pursued:

We start with a laminar simulation and a first order upwind scheme only for the momentum equation and switch to second order accuracy after a few iterations. With this initial guess we solve the fluid and temperature fields by using the SST-kω turbulence model that is implemented in Fluent. All equations are solved with second order accuracy.

With this approach it is possible to achieve a stationary solution. The greatest problem as far as convergence is concerned is the accurate prediction of the separation eddies occurring behind the last tube row.

The steady result of the 2D simulation is compared with PIV data obtained at wall distance $z/b_{1/2}$=1, i.e. in the middle of the flow passage between the two fins. This comparison is justified because the flow in the mirror plane of the flow channel is quasi two–dimensional as proven by examination of the residua of the continuity equation calculated from PIV data.

The result of the 2D simulation is displayed in Figure 4**.** It agrees well with the mean velocity field of the PIV measurements. According to the experimental results the streamlines do not join adjacent wave like flow channels as discussed in the previous section.

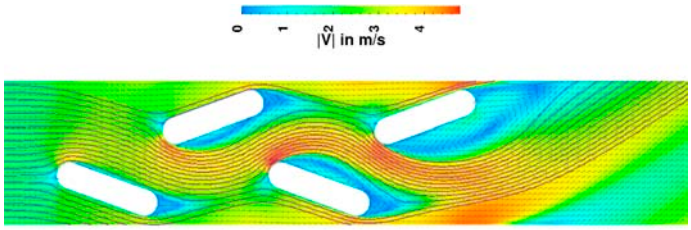

Figure 4 Steady 2D numerical solution of the flow field in a periodic model of the flat tube heat exchanger at Re_{dh}=3900.

The comparison of the crucial separation eddy behind the last tube row is shown in greater detail in Figure 5. We find a slight difference in the shape of the wake region behind the last tube row. In the numerical solution it extends into +y–direction indicated by the upwards bended vorticity streaks. The flow experiment, however, shows a slight bending downwards into -y–direction.

This deviation is most likely owed to the wall influence of an additional Perspex wall at $y=2.5s_q$ which is only present in the experimental model. Contrarily, the numerical model assumes full periodicity in y–direction.

The calculated pressure drop across the flat tube geometry is also compared to the experimental monitoring of this quantity. The numerical prediction yields a drop of the static pressure of Δp_{num}=8.7Pa whereas the measurement during PIV runs shows a pressure drop of Δp_{exp}= (9.5±0.2)Pa. This is an agreement within 9%. It is reasonable that the numerical solution predicts a lower pressure drop since it solves a purely two dimensional flow with no fins confining the flow in z-direction. Thus, we do not have additional boundary layers that cause additional pressure losses.

These results qualify the numerical model as a suitable candidate for a 2D optimization process as described in [2].

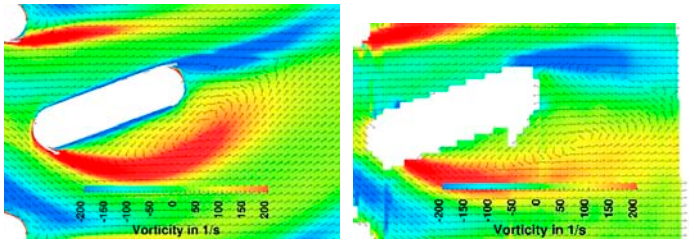

Figure 5 Comparison of the vorticity downstream the last tube row (tube 1-4) between numerical simulation (left) and PIV measurement (right).

COMPARISON OF HEAT TRANSFER AND FLUID FLOW

In addition to the fluid flow the heat transfer distribution in the named flat tube heat exchanger is studied at Re_{dh}=2500. The experimental analysis is done by means of the ammonia absorption method (AAM) [3]. This mass transfer measurement technique uses a color reaction between ammonia injected into the air flow and manganese chloride applied with the help of filtering paper to the heat transfer surface. The reaction product is MnO_2 which has a brownish color. Its color intensity is a direct measure of the amount of ammonia transferred onto the thus prepared surface. During post processing the method employs the analogy between heat and mass transfer and a calibration procedure relying on literature correlations [4].

The advantage of this method is the relatively high spatial resolution. Structures in the order of 1mm can easily be distinguished. This resolution is not limited by the size of the measurement area. A whole heat exchanger can be analyzed with the same resolution.

The local distribution of the dimensionless heat transfer coefficient on the fin is displayed in Figure 6.

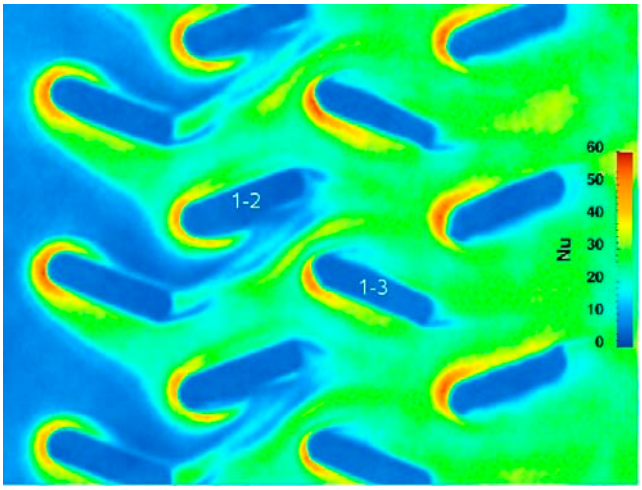

Figure 6: Map of the local heat transfer distribution on the fin of the flat tube heat exchanger at Re_{dh}=2500 measured by AAM.

It shows continuously increasing heat transfer values in downstream direction. This indicates that we do not achieve fully developed conditions within four tube rows.

Horseshoe vortices characterized by enhanced heat transfer rates form at each tube row. Due to the inclination of the tube those vortices are asymmetric.

In the middle of the geometry, namely between tube 1-2 and 1-3 the heat transfer distribution is quite complicated. We find a long streak of enhanced heat transfer that cannot be associated with horseshoe vortices. This region is studied in greater detail and also analyzed in conjunction with near wall and high resolution PIV measurements.

The named region is shown in an enlarged picture in Figure 7. The left picture shows the heat transfer distribution and the right picture a map of the quantity $\partial W/\partial z$ determined from PIV measurements. This quantity is determined under the assumption of incompressible flow for which the equation of continuity $\vec{\nabla} \cdot \vec{u} = 0$ holds. It can be calculated from two dimensional PIV velocity fields as the negative residue of this equation. For this reason it is clear that $\partial W/\partial z$ is a measure of the three dimensional character of the flow. In regions of large positive or negative values of $\partial W/\partial z$ we have a strong out–of–plane movement of fluid which is favorable for heat transfer to the fins. The PIV measurement shown in Figure 7 has been made at very close wall distance of $z/b_{1/2}$=0.5 corresponding to z=0.5mm.

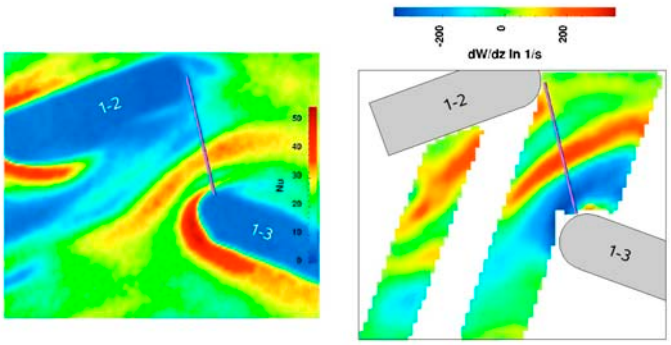

Figure 7 Comparison of characteristic features in the heat transfer distribution (left) and in the ∂W/∂z map measured at a wall distance of $z/b_{1/2}$=0.5 (right). The pictures show the region between tube 1-2 and 1-3 at a Reynolds number of Re_{dh}=2500.

The comparison shows that the streak of enhanced heat transfer has a very similar counterpart in the ∂W/∂z map. We clearly find this structure as a streak of high values of the residue in the right picture of Figure 7.

A quantitative comparison confirms this assumption. The heat transfer values as well as the ∂W/∂z values are extracted along a line indicated in Figure 7**.** Both quantities are plotted against the distance along the scan line (cf. Figure 8).

The region of large positive and negative ∂W/∂z values between x/L=0 and x/L=0.6 correspond quite well with a pronounced heat transfer.

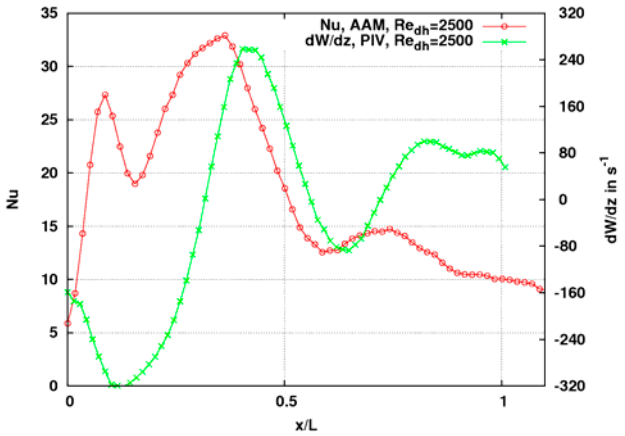

Figure 8 Comparison of heat transfer values and the flow quantity ∂W/∂z extracted along a line between two flat tubes. Large values of ∂W/∂z correspond to an enhanced heat transfer.

RECONSTRUCTION OF GAPPY PIV DATA

The gappy POD has first been proposed by Everson and Sirovich [5] in the field of face recognition. Thanh et al. have extended this procedure to fluiddynamical problems involving the reconstruction of velocity and pressure fields around airfoils [6]. An analysis of the reliability and applicability of the gappy POD has been presented by Venturi and Karniadakis [7]. They also proposed a scheme to avoid the dependence of the repaired data on the initial guess of missing data. Recently, a direct application to 2D PIV measurements in a rectangular cavity flow with a low degree of gappiness has been reported by Murray and Ukeily [8].

In this paper we follow the procedure described by Everson and Sirovich. This is an iterative scheme combining a standard POD method and a fit process during the reconstruction process.

The shadowed regions are considered as missing data spots. If we apply k different light sheet angles to the same measurement region Ω we are usually faced with a total of k different shadow masks. Each mask $m_n(\vec{x})$ describes whether a point $\vec{x}$ carries valid data. All measurements of the region Ω resulting from different illuminations contribute to the total gappy ensemble consisting of M gappy velocity fields

$$\left\{\mathring{\vec{u}}_n(\vec{x})\right\}_{n=1}^{M} \quad \text{where} \quad \mathring{\vec{u}}_n(\vec{x}) = m_n(\vec{x})\vec{u}_n(\vec{x}).$$

The mask function $m_n(\vec{x})$ has either the value 0 if there is no information at $\vec{x}$ or 1 if there is valid data at $\vec{x}$.

In the first step of the Everson–Sirovich procedure the obscured spots are filled by average data from the other light sheet angles. The average value is defined as

$$\left\langle \mathring{\vec{u}}_n(\vec{x}) \right\rangle = \frac{1}{N(\vec{x})} \sum_{n \in G[\vec{x}]} \mathring{\vec{u}}_n(\vec{x})$$

with $G[\vec{x}]$ being the set of all indices n for which $m_n(\vec{x}) = 1$ and $N(\vec{x})$ being the number of valid data values at the given location $\vec{x}$. These averaged values are used to fill the missing data in a rather crude first guess. We obtain the initial approximated ensemble:

$$\left\{\tilde{\vec{u}}_n^{(0)}(\vec{x})\right\}_{n=1}^{M}$$

Now, a standard snapshot POD (cf. [9]) is performed with this velocity ensemble. The thus obtained spatial basis functions $\vec{\varphi}(\vec{x})$ are used to reconstruct the missing data in order to get a better approximation than in the initial step. The core of the reconstruction process is the calculation of approximate values $\hat{\vec{u}}_n$ as a finite expansion in terms of the spatial POD basis functions:

$$\hat{\vec{u}}_n^{(i+1)}(\vec{x}) = \sum_{j=1}^{R} \tilde{a}_j^{(i+1)}(n)\ \tilde{\vec{\varphi}}_j^{(i)}(\vec{x})$$

The determination of the coefficients $\tilde{a}_j^{(i+1)}$ is done through a fitting process described in [5]. The values $\hat{\vec{u}}_n^{(i+1)}$ are inserted only at locations where $m_n(\vec{x}) = 0$. At all other locations we can use the measured data and thus form the (i+1)–th approximated ensemble

$$\left\{\tilde{\vec{u}}_n^{(i+1)}(\vec{x})\right\}_{n=1}^{M}.$$

After this reconstruction we proceed with the next iteration step, namely a POD analysis of the functions $\tilde{\vec{u}}_n^{(i+1)}$ and continue until convergence is achieved (cf. [5]).

The afore described procedure is performed on a data set consisting of three different light sheet positions, i.e. three different masks $m_n(\vec{x})$. The region containing valid data is illustrated in Figure 9. Each of the colored areas is associated with valid data of a certain light sheet. The superposition of the three areas defines the measurement region Ω.

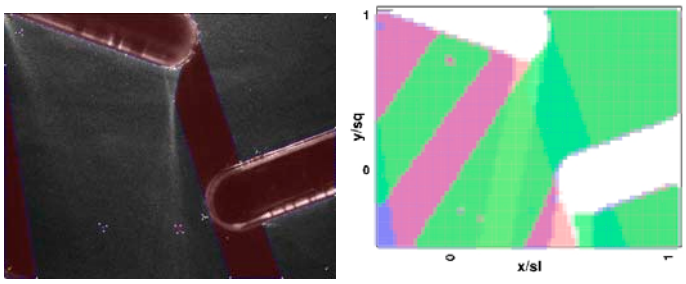

Figure 9: Illustration of the shadowed regions (left) and of the valid PIV data associated with each light sheet (right). The three colored areas (red, green and blue) visualize the pixels at which unobscured velocity data has been obtained.

The outcome of the gappy POD procedure are approximate instantaneous velocity fields for the whole measurement region Ω. A typical instantaneous velocity field reconstructed by the here described procedure is shown in the left picture of Figure 10. Within the iteration process we have used the first five POD basis functions for the reconstruction (R=5). The properties of the POD ensure that the approximation is optimal in a least square sense [10].

In order to judge about the quality of the reconstruction a reference measurement has been done with a different light sheet angle thus covering only a certain area Ω_{ref} of Ω $\left(\Omega_{ref} \subset \Omega\right)$. The reconstructed instantaneous velocities $\tilde{\vec{u}}_n$ are subtracted from the reference velocities $\vec{u}_{n,ref}$ at all $\vec{x} \in \Omega_{ref}$. The magnitude of the deviation vector is visualized in Figure 10 to get a rude estimation of the reliability of the procedure**.**

The average deviation is about 0.09m/s. This is a difference of about 3.5% compared to the measured mean velocity in Ω_{ref}.

This very first result is an encouraging step towards a reliable reconstruction of marred instantaneous velocity fields in the PIV analysis of complex geometries like heat exchangers.

Future work has to be done to judge whether the achieved reconstruction is indeed the best reconstruction. The double iterative procedure proposed by Venturi and Karniadakis will be a valuable scheme for further investigation of this matter.

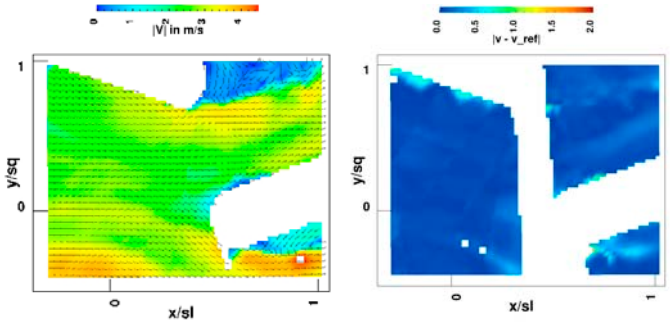

Figure 10 Typical reconstructed instantaneous velocity field (left) and map of the deviation between reconstructed and reference field $\left|\tilde{\vec{u}}_n - \vec{u}_{n,ref}\right|$.

CONCLUSIONS

The flow field as well as the heat transfer distribution is studied in flat tube heat exchangers with inclined refrigerant tubes and plane fins at Re_{dh}=3900 and Re_{dh}=2500.

The PIV analysis in the symmetry plane of the flow passage shows the fluid moving in a wave like channel between the tubes with a small lateral component. The behavior changes in a plane close to the wall where the fluid exhibits a strong lateral movement promoting lateral mixing of fluid.

The measured flow field in the symmetry plane has also been modeled by a stationary 2D CFD simulation using a k–ω turbulence model. The validated model can be used for further geometrical optimization tasks.

A combined analysis of local heat transfer distribution on the fin and near wall PIV measurements reveals a clear relation between strong three dimensional flow seen in the PIV measurements and an enhanced heat transfer. We find very similar structures in the heat transfer map as well as in the map of the residue of the equation of continuity.

Flow measurements by means of PIV are hindered in the named geometries by shadows yielding missing or invalid data. Instantaneous velocity fields can be reconstructed using the gappy POD procedure. Shadowed regions are filled by approximated data. Comparison with reference data shows an average deviation of about 3.5% of the reconstructed velocity fields.

REFERENCES

[1] Ahrend U., Buchholz M., Schmidt R., Koehler J., Investigation of The Relation Between Turbulent Fluid Flow And Local Heat Transfer in Fin–And–Tube Heat Exchangers, *Proc. IHTC 13,* Sydney, Australia, 2006

[2] Correia C, Bockholt M., Tegethoff W., Koehler J., Geometry Optimization of Louvered Fins for a Compact Flat Tube Heat Exchanger, *Proc. CMNE/CILAMCE 2007*, Porto, Portugal, 2007

[3] Kottke, V., Blenke, H., Schmidt, K. G., Eine remissionsfotometrische Messmethode zur Bestimmung oertlicher Stoffuebergangskoeffizienten bei Zwangskonvektion in Luft, *Waerme- und Stoffuebertragung / Thermo- and Fluiddynamics*, Vol. 10, pp. 9-21

[4] Ahrend U., Freund S., Henze M., Koehler J., Experimental and Numerical Investigations of Heat Transfer in Complex Internal Flows with Vortex Inducing Elements − Introduction to a Joined Project and Typical Results, *Proc. of Int. Conf. Comp. Heat Exchanger,* Potsdam, Germany, 2007

[5] Everson R., Sirovich L., Karhunen–Loeve Procedure for Gappy Data, *J. Opt. Soc. Am. A,* Vol. 12, No. 8, 1995

[6] Bui–Thanh T., Damodaran M., Willcox K., Aerodynamic Data Reconstruction and Inverse Design Using Proper Orthogonal Decomposition *AIAA Journal,* Vol. 42, No. 8, 2004

[7] Venturi D., Karniadakis G.E., Gappy Data and Reconstruction Procedures for Flow Past a Cylinder, *J. Fluid Mech.,* Vol. 519, pp. 315-336, 2004

[8] Murray N.E., Ukeiley L.S., An Application of Gappy POD for Subsonic Cavity Flow Data, *Exp. Fluids*, Vol. 42, pp. 79-91, 2007

[9] Sirovich L., Turbulence And The Dynamics Of Coherent Structures Part I-III, Quaterly Of Applied Mathematics, Vol. XLV, No. 3, pp. 561-590, 1987

[10] Holmes P., Lumley J.L., Berkooz G., Turbulence, Coherent Structures, Dynamical Systems and Symmetry, *Cambridge University Press,* Cambridge, U.K., 1996